Eva K. B. Pfannes | Alexander Anielski | Matthias Gerhardt
Carsten Beta

Intracellular photoactivation of caged cGMP induces myosin II and actin responses in motile cells

Suggested citation referring to the original publication:
Integrative biology 5 (2013), pp. 1456–1463
DOI http://dx.doi.org/10.1039/c3ib40109j

Integrative Biology

RSC Publishing

PAPER

View Article Online
View Journal | View Issue

Intracellular photoactivation of caged cGMP induces myosin II and actin responses in motile cells†

Cite this: *Integr. Biol.*, 2013, **5**, 1456

Eva K. B. Pfannes, Alexander Anielski, Matthias Gerhardt and Carsten Beta*

Received 31st May 2013,
Accepted 29th September 2013

DOI: 10.1039/c3ib40109j

www.rsc.org/ibiology

Cyclic GMP (cGMP) is a ubiquitous second messenger in eukaryotic cells. It is assumed to regulate the association of myosin II with the cytoskeleton of motile cells. When cells of the social amoeba *Dictyostelium discoideum* are exposed to chemoattractants or to increased osmotic stress, intracellular cGMP levels rise, preceding the accumulation of myosin II in the cell cortex. To directly investigate the impact of intracellular cGMP on cytoskeletal dynamics in a living cell, we released cGMP inside the cell by laser-induced photo-cleavage of a caged precursor. With this approach, we could directly show in a live cell experiment that an increase in intracellular cGMP indeed induces myosin II to accumulate in the cortex. Unexpectedly, we observed for the first time that also the amount of filamentous actin in the cell cortex increases upon a rise in the cGMP concentration, independently of cAMP receptor activation and signaling. We discuss our results in the light of recent work on the cGMP signaling pathway and suggest possible links between cGMP signaling and the actin system.

Insight, innovation, integration

Second messengers like cGMP play a central role in the regulatory pathways of living cells. Here, we demonstrate that an increase in intracellular cGMP can trigger not only myosin II but also actin responses in motile amoeboid cells. In previous studies, an increase in intracellular cGMP was induced indirectly *via* membrane receptor stimulation. In the present work, we employ, for the first time, the direct light-induced release of cGMP from a caged precursor to raise the cytosolic cGMP level in *Dictyostelium* cells that carry fluorescent markers for filamentous actin and myosin II. Based on this advanced combination of live cell photo-uncaging and multi-color confocal microscopy, we could identify a link between cGMP and actin dynamics in motile amoeboid cells.

Introduction

Cell motility and chemotaxis are fundamental to living organisms. They are the underlying key mechanisms of a wide variety of biological processes, including embryonic morphogenesis, cancer metastasis, and wound healing. In eukaryotic cells, motility is mostly driven by the dynamics of the actin cytoskeleton. Under the influence of an external chemical gradient, the symmetry of the actin cortex breaks into a leading edge and a retracting tail. While the leading edge is dominated by actin polymerization and the presence of filament nucleators like the Arp2/3 complex, the tail exhibits accumulation of myosin II, a well-known motor protein that generates contractile forces in conjunction with actin filaments.[1] One of the most prominent eukaryotic model organisms to study the role of cytoskeletal proteins and regulators in actin-driven motility is the social amoeba *Dictyostelium discoideum.*[2] Vegetative *Dictyostelium* cells show directional responses to gradients of folic acid. When starved for several hours, a signaling system is expressed that mediates chemotaxis in gradients of extracellular cAMP.[2]

When exposed to cAMP, starvation-developed *Dictyostelium* cells display a cascade of signaling events that lead to a sharp and transient increase in actin polymerization within the first 10 s following the stimulus, accompanied by the cortical localization of associated regulatory proteins. With a delay of about 20 s, the actin response is followed by a prolonged accumulation of myosin II in the cell cortex.[3] Along with these cytoskeletal rearrangements, also a transient 10-fold increase in the cytosolic level of cGMP is observed.[4] The intracellular cGMP concentration peaks after 10 s and decays back to basal levels after about 30 s.[5,6] In the KI-8 and KI-10 chemotaxis defective mutants, no such increase in the intracellular cGMP concentration was observed and, in addition, no recruitment of myosin II to the cell cortex.[4] On the other hand, the streamer

Biological Physics, Institute of Physics and Astronomy, University of Potsdam, Karl-Liebknecht-Str. 24/25, 14476 Potsdam, Germany. E-mail: beta@uni-potsdam.de; Fax: +49 331 977 5617; Tel: +49 331 977 5653

† Electronic supplementary information (ESI) available. See DOI: 10.1039/c3ib40109j

F mutant (stmF) shows a prolonged increase in cGMP levels in response to a chemoattractant stimulus. This is associated with a much longer association of myosin II with the cytoskeleton, an extended phase of elongation during chemotaxis,[7–9] and a delay in the phosphorylation of the myosin II light chain.[10] Together, these early results suggest that cGMP plays a central role in controlling the phosphorylation and cytoskeletal localization of myosin II.

In *Dictyostelium*, cGMP is synthetized by membrane-bound guanylyl cyclase A (GCA) and by soluble guanylyl cyclase (sGC).[11] Both GCA and sGC are activated in live cells by chemoattractant stimulation.[12] Similarly, osmotic stress also activates guanylyl cyclase in *Dictyostelium.*[13,14] Only a small amount of the produced cGMP is secreted, the major part is degraded by a cGMP specific phosdiesterase (PDE). Effects of extracellular cGMP on the chemotactic signaling system of *Dictyostelium* are about 1000-fold lower than those of cAMP.[15] Cyclic GMP production appears to be regulated by Ras subfamily GTPases. The small GTPase Rap1 promotes cGMP production in osmotic stress. Rap1 controls cell adhesion in mammalian cells and was shown to regulate cell polarity and motility by controlling myosin II function in *Dictyostelium.*[16] In metazoans, cGMP binds to cGMP-dependent protein kinases (PKGs), cGMP gated ion channels, cAMP/cGMP-regulated Ras and cGMP-regulated phosphodiesterases.[16,17] In *Dictyostelium*, four putative cGMP-binding proteins (GbpA-D) have been identified.[18] The cGMP binding protein A (GbpA) is a cGMP-specific PDE that is activated by cGMP, while GpbB, a dual specificity PDE with a preference for cAMP, is activated by both cAMP and cGMP.[18,19] Furthermore, the two large multi-domain proteins GbpC and GpcD have been characterized.[12]

It was found that GbpD acts independently of intracellular cyclic nucleotides. It promotes surface attachment *via* lateral pseudopods and depolarization as part of a GbpD/Rap/PI3K pathway.[20,21] GbpC, on the other hand, exhibits a high cGMP binding affinity. It is considered to be the only cGMP signal-transducing protein in *Dictyostelium*. Activation of GbpC by cGMP is essential for myosin II regulation during chemotaxis, multicellular streaming, and resistance to osmotic stress.[12,22] Subsequent studies revealed a rich topology of domains that led to the classification of GbpC as a member of the Roco family of proteins.[23] A multi-step intramolecular activation mechanism has been identified for this protein[24,25] and its subcellular localization in response to cAMP-stimuli and osmotic shock was studied.[26] Despite our detailed mechanistic knowledge of GbpC activation, many open questions remain. In particular, the substrates that are phosphorylated by active GbpC in the cell cortex remain so far unknown. Myosin II assembly relies critically on these processes. But also other cortical functions may be triggered *via* this pathway.

Most of our knowlegde on biochemical pathways like the cGMP signaling network relies on a combination of mutant studies and conventional biochemical assays. The response to an input stimulus (rise in extracellular cAMP concentration, osmotic shocks) is characterized at various levels, for example, cell shape, cellular functions, changes in the concentration levels of intracellular components, in their localization, their degree of phosphorylation *etc.* Already more than two decades ago, such studies have led to the conjecture that cGMP is essential for controling myosin II function in *Dictyostelium*. A major complication of this approach arises from the fact that in eukaryotic cells, an external stimulus often triggers multiple pathways that may act in parallel and interfere with each other. In order to unambiguously demonstrate the action of individual players in a signaling cascade, it is necessary to directly manipulate their intracellular concentration levels by artificially introducing them into the cell in a controlled manner. In many cases, this is difficult to achieve, if not impossible. A number of different approaches like microinjection and induced gene expression have been developed to achieve this goal. Among them, membrane permeable caged compounds offer some of the most promising options for precise temporal delivery of molecules inside cells. Upon photo-activation, such compounds release the desired signaling substance from a biochemically inert caged precursor—an approach that has evolved into one of the most versatile tools for chemical stimulation in live cells.[27]

Almost all classes of biologically relevant signaling molecules have been produced in caged versions, including molecules of very different sizes like Ca^{2+}, nucleotides, and inositols but also mRNA, DNA, peptides, and enzymes. Prominent examples of the use of caged compounds range from the study of ion channels to secretory processes and glutamate receptor stimulation. For a review see ref. 28 and further references therein.

In the present work, we will use a membrane permeable caged version of cGMP to directly investigate the impact of a sudden increase in intracellular cGMP on the cytoskeletal dynamics of *Dictyostlium* cells. In particular, we will study the temporal responses in cortical actin polymerization and myosin II localization by dual color fluorescence imaging of a *Dictyostelium* cell line that carries fluorescent markers for both filamentous actin and myosin II. We furthermore explore the effect of different placements of the uncaging laser in the field of view (inside the cell of interest *versus* outside next to the cell of interest) and analyze to what extent stray light limits localized photo-uncaging.

Results

Both actin and myosin II respond to a light-induced release of cGMP

Intracellular photo-activation of caged cGMP was carried out in *Dictyostelium* cells that co-expressed LimEΔ-mRFP and myosin-II-GFP. LimEΔ-mRFP, the fluorescently tagged version of a *Dictyostelium* Lim-domain protein with truncated coiled-coil domain, is a well-established marker for filamentous actin.[29] Together with the GFP-tagged version of myosin II, the intracellular acto-myosin distribution was directly recorded in live cells by fluorescence microscopy. Images were taken by dual-color confocal laser scanning microscopy, so that both labels were simultaneously followed in the same cell. In Fig. 1A and C, the snapshot of a single non-stimulated cell is displayed as an example, with the LimEΔ distribution in red (A) and the myosin II distribution in green (C).

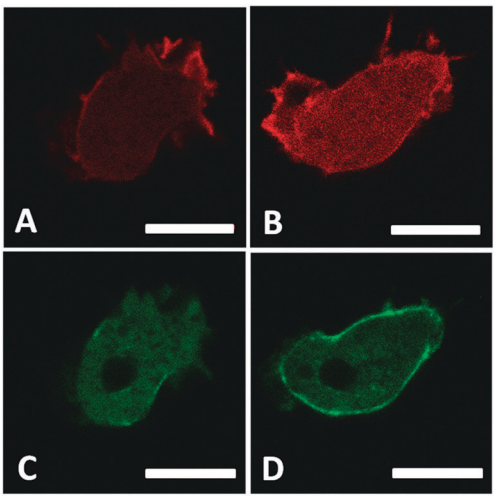

Fig. 1 Examples of confocal images of vegetative *Dictyostelium* cells expressing LimEΔ-mRFP and myosin II-GFP. LimEΔ-mRFP distribution (A) before and (B) 12 s after intracellular release of cGMP. Myosin II-GFP distribution (C) before and (D) 15 s after intracellular release of cGMP. Scale bar corresponds to 10 μm.

Prior to the uncaging experiment, we incubated the cells with a membrane permeable caged version of cGMP (DMACM-caged cGMP). Each cell was recorded for at least 100 s. After 20 s, we initiated uncaging by a short 1 s pulse delivered with a 405 nm laser. In Fig. 2A, the light-induced uncaging reaction is displayed. Two different types of uncaging experiments were carried out,

- the uncaging laser was positioned inside the cell of interest;
- the uncaging laser was positioned outside, a distance of about 5 μm away from the cell of interest.

In Fig. 2B and C, the two situations are depicted schematically. We performed both types of experiments with vegetative as well as with starvation-developed cells. For each scenario, a large number of single cell recordings were taken (between 19 and 77, see the caption of Fig. 3 for details). Moreover, we took the respective controls for each case that consisted of a recording under identical conditions without the uncaging event.

When placing the uncaging laser inside vegetative cells, we observed both a clear myosin II response and also an actin response. Examples are shown in Fig. 1B and D, respectively. In both cases, an increased localization of the fluorescent fusion protein was seen in the cell cortex following the uncaging event. To quantify the time course of the response, we divided the cell area into a cortical and a cytosolic region and determined the average fluorescence intensities in both regions for each time frame. In Fig. 2D, the masks for image segmentation and differentiation of cortex and cytosol are shown (see also the Methods section below). For a detailed description of the image analysis please refer to Anielski *et al.*[31] Upon translocation of fluorescent fusion proteins from the cytosol to the cortex, the average cytosolic fluorescence intensity decreased, while the cortical fluorescence intensity was at the same time increasing. In Fig. 3, we plot the ratio of the cortical and the cytosolic fluorescence intensities. The signals for both actin (black) and myosin II (red) are shown. The average response of vegetative cells that were stimulated by placing the uncaging laser inside the cell can be seen in Fig. 3A. Both the actin and the myosin II-peak are clearly visible. We observed that actin peaked within the first 10 s after the uncaging event, while cortical myosin II localization reached its maximum about 30 s after uncaging.

When placing the uncaging laser outside at a distance of about 5 μm away from the cell of interest, vegetative cells still showed an actin response, while no clear myosin II translocation to the cortex was observed. This can be seen in Fig. 3C, where the corresponding time traces for the ratio of cortical and cytosolic

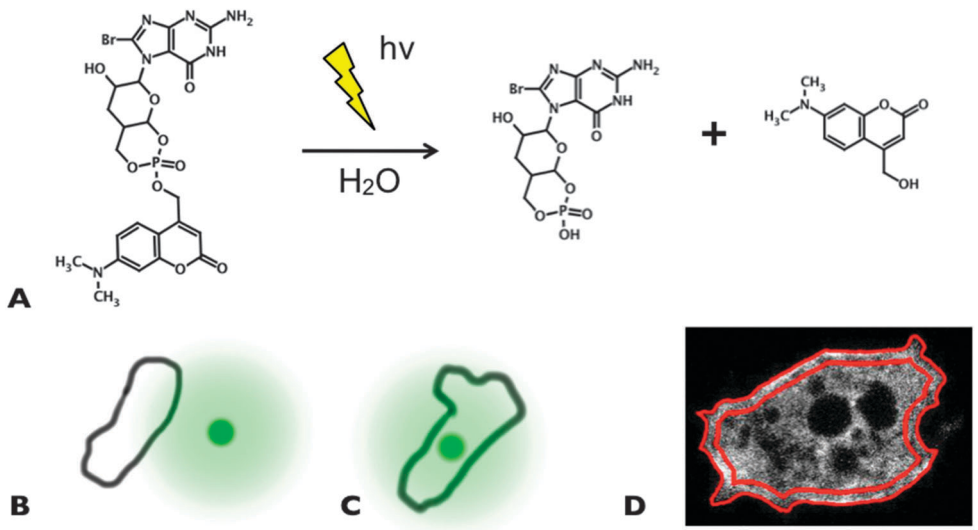

Fig. 2 Uncaging of DMACM-caged 8-Br-cGMP. (A) Structure of DMACM-caged 8-Br-cGMP and the release of Br-cGMP, based on Hagen *et al.*[30] Configurations for (B) placing the uncaging laser outside and (C) placing the uncaging laser inside the cell. Note that although the laser is focused to an uncaging region of a circle with 1.071 μm (21 pixels) diameter, stray light can still cause uncaging inside neighboring cells. In D, masks generated for image analysis are shown in red. Adapted from Anielski *et al.*[31]

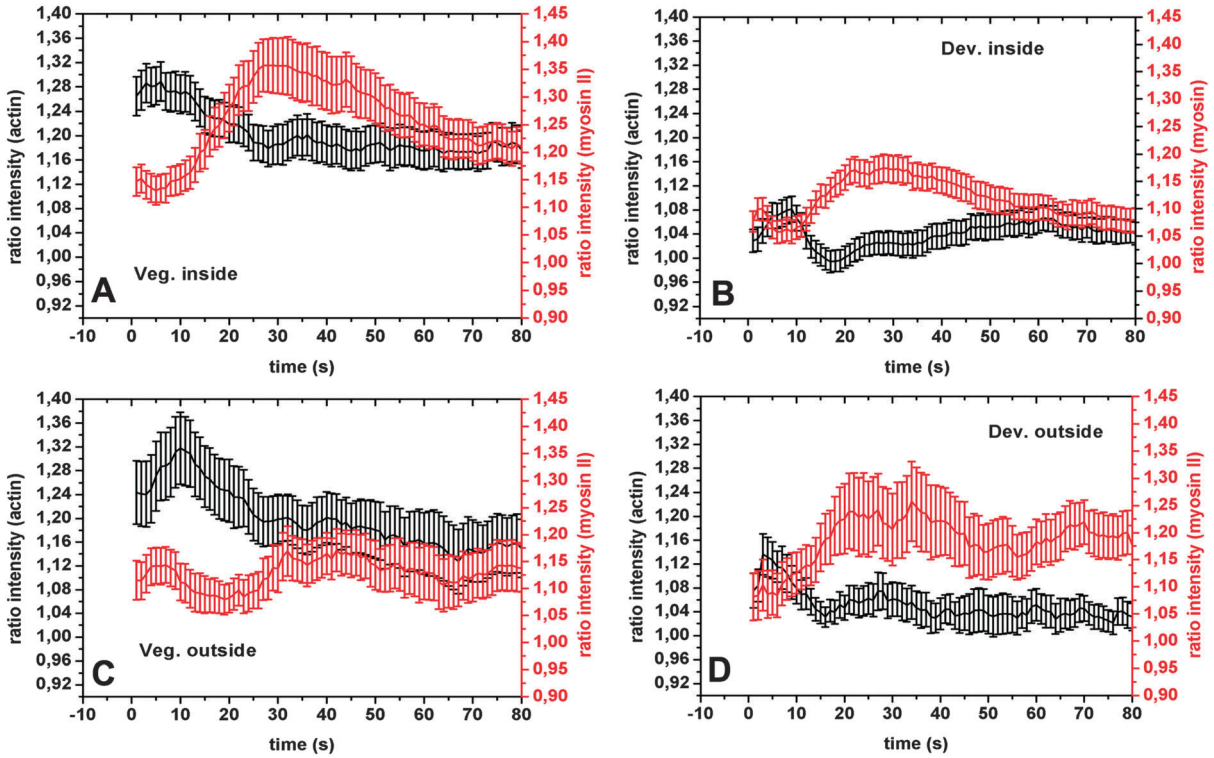

Fig. 3 Actin and myosin II response curves, for vegetative and starvation developed cells, incubated with DMACM-caged cGMP. The vertical axis on the left (black) always shows the values for the actin curve, the vertical axis on the right (red), the values for myosin II. The stimulus was delivered at $t = 0$. Error bars indicate the standard error. (A) Actin and myosin II curves of vegetative cells, when placing the uncaging laser inside the cell. Number of cells analyzed: 45 for actin and 47 for myosin II. (B) Actin and myosin II responses of developed cells when placing the uncaging laser inside the cell. Number of cells analyzed: 74 for actin and 77 for myosin II. (C) Actin and myosin II curves of vegetative cells, when placing the uncaging laser outside the cell. Number of cells analyzed: 25 for both actin and myosin II. (D) Actin and myosin II responses of developed cells when placing the uncaging laser outside the cell. Number of cells analyzed: 19 for actin and 21 for myosin II.

fluorescence intensities are displayed. For starvation-developed cells, a similar response was observed when placing the uncaging laser inside the cell. Both actin and myosin II accumulated in the cell cortex, following an intracellular release of cGMP. Also the timing of the actin and myosin II peaks was similar to the dynamics observed in vegetative cells, see Fig. 3B. In contrast to the results for vegetative cells, starvation developed cells showed not only an actin response, but also a clear myosin II translocation upon illumination of an uncaging region placed outside of the cell, see Fig. 3D.

We have performed a number of control experiments to verify that the observed responses are indeed caused by the light-induced release of cGMP. Besides (1) control recordings of cells that are neither exposed to caged cGMP nor to the uncaging light, we have (2) incubated cells in the caged compound without exposure to the uncaging light, and (3) exposed cells to the uncaging light in the absence of the caged compound. In none of these cases, significant responses were observed. The results are displayed in the ESI.†

Cytoskeletal responses are triggered by intracellular uncaging of cGMP

How can we explain that for both types of photo-uncaging experiments (placing the uncaging laser inside/outside of the cell) responses in the cortical dynamics were observed? We envision two possible scenarios. (1) The cortical responses are induced by extracellular cGMP *via* a receptor pathway. This would immediately explain the responses in cases where the uncaging laser is placed outside the cell. But also responses for uncaging inside the cell could be explained in this way. The cells were surrounded by a solution of caged cGMP. After passing through the cell, the laser also exposed the extracellular medium beyond the cell to the UV light, thus releasing a certain amount of cGMP in the vicinity of the cell. (2) The cortical responses are induced by intracellular cGMP. This would explain the responses in cases where the uncaging laser is placed inside the cell. The responses in cases where the uncaging laser was placed outside the cell could be attributed to stray light effects (secondary uncaging events). Small impurities and dust particles on the cover slip and in the surrounding solution may scatter light from the initial path of the laser beam into other directions, some of them inducing uncaging events inside neighbouring cells.

To discriminate between the two possible scenarios, we first performed extensive controls to make sure that the responses we observed in the acto-myosin system were not triggered by extracellular cGMP. In particular, we have performed micropipette aspiration experiments to expose cells from the outside to cGMP, Br-cGMP, and 7-dimethylamino-4-methyl-coumarin (DMAC), an analogue of the cage that was used in our uncaging experiments.

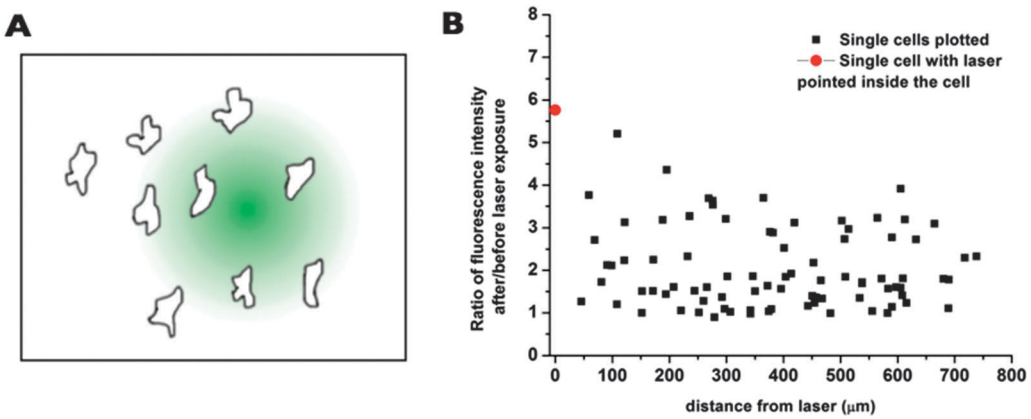

Fig. 4 Dihydroethidium photoactivation assay. In (A), a schematic of the experiment is shown, with cells distributed over the field of view and the laser pointing to a position in between the cells. Fading color indicates the stray light. In (B), each square in the plot represents a cell and its corresponding ratio of the fluorescence intensities before and after the photo-activation. The circle in red represents a cell that is directly hit by the laser. Cells up to a distance of 750 μm from the laser source were quantified. Cells from three independent experiments are included.

The results from these control experiments can be seen in the ESI.† In none of these cases, actin or myosin responses were observed. This clearly demonstrates that the responses presented in Fig. 3 were caused by the light-induced release of cGMP inside the cell, thus favouring scenario (2). To confirm this, we have performed a separate series of experiments that is described in the following.

Stray light induces secondary uncaging inside cells that are not directly targeted by the UV laser

To monitor the amount of uncaging light that reaches cells during an uncaging experiment, we used Dihydroethidium, a fluorescent reporter that was recently introduced by Brasen *et al.* to quantify the UV intensity delivered to the cytosol of cells in an uncaging experiment.[32] Dihydroethidium is a membrane permeable compound that can be photo-oxidated to hydroxyethidium when exposed to UV light. Hydroxyethidium is fluorescent and membrane impermeable.[32] For our study AX2 wild type cells were plated in glass-bottom Petri dishes and incubated for 2 hours in 20 μM Dihydroethidium under protection from light. We then exposed individual cells to the light of a focused 355 nm laser (Fig. 4A) and measured the intracellular fluorescence of hydroxyethidium before and after UV exposure. In addition, intracellular fluorescence was also measured in cells, which were not in the focus of the uncaging laser. The intracellular fluorescence of hydroxyethidium in individual cells is plotted as a function of the distance from the focus of the laser in Fig. 4B. The data clearly show that after direct exposure of a cell to the uncaging laser, the fluorescence of hydroxyethidium increases intracellularly as expected. Interestingly also in cells with a distance of several 100 micrometers away from the laser focus significant intracellular fluorescence of hydroxyethidium was found. Furthermore, it can be seen that in cells not directly exposed to the laser beam, the degree of intracellular photoactivation scattered over a wide range. In most cases, the secondary photoactivation events reached levels of up to 50% or less compared to photoactivaion in cells directly hit by the uncaging laser. Also, up to about 1 mm, the degree of secondary photoactivation showed only a weak dependence on the distance from the light beam.

These results clearly favor scenario (2) to explain the cortical responses in experiments, where the uncaging laser was placed outside the cell. Light from the uncaging laser may be scattered by small impurities and dust particles. In particular, in cases where the uncaging laser passed directly through a cell, small structures and inhomogeneities in the cytosol will scatter light off the initial direction of the laser beam into the surroundings of the cell. This stray light will induce secondary intracellular photoactivation in neighbouring cells that are not directly exposed to the uncaging laser, see the schematic representation of this process in Fig. 4A. The large spread of the data points displayed in Fig. 4B reflects that the distribution of stray light is strongly anisotropic, depending on the number, shape, and orientation of the scattering objects. In general, our results demonstrate that secondary uncaging by stray light may strongly influence the results of intracellular uncaging experiments. Thus, possible side effects of secondary uncaging should be considered whenever photo-uncaging is used for stimulation in living cells.

On the other hand, we may employ secondary uncaging to deliberately reduce the UV exposure of cells during an uncaging experiment because, on average, secondary uncaging is significantly weaker than the primary uncaging event. Consequently, also the intracellular photo-release – in our case of cGMP – will be lower in this setting. We may thus interpret the difference observed in Fig. 3C and D between vegetative and starved cells as follows. In vegetative cells, a reduced dose of cGMP elicits only actin responses, indicating that cortical myosin localization in vegetative cells is less sensitive to changes in intracellular cGMP levels than actin.

Discussion

We exposed vegetative and starvation developed *Dictyostelium* cells to a sudden increase in the cytosolic cGMP concentration.

The stimulus was delivered by light-induced intracellular release of a photo-activatable caged version of cGMP. In general, the most widely used caged compounds are based on a nitrobenzyl group that can be activated by UV light.[27] Photochemical activation may be a single-cycle process, when irradiation of the photocleavable functional group causes activation, or even a multicycle process, when biologically inactive and active states can be acessed and reversed with different wavelenghts.[33] For extracellular stimulation of *Dictyostelium* cells with complex and rapidly switching signals, the light-induced release of such compounds was successfully demonstrated.[34,35] In the present work, we used the [7-(dimethylamino)coumarin-4-yl]methyl (DMACM) ester of 8-Br-cGMP, a photolabile cGMP analogue that is known to be membrane permeable, poorly hydrolyzed by phosphodiesterases, stably soluble in aqueous buffer solution, and rapidly released upon illumination.[30] Compared to the nitrobenzyl derivatives, optimal photocleavage of this compound is shifted to longer wavelengths (330–440 nm, λ_{max} 398 nm), reducing cell damage and photo-bleaching.[30,36,37]

In our intracellular photo-activation experiments, we observed that an increase in the intracellular level of cGMP elicits a response in both actin polymerization and cortical localization of myosin II filaments. While actin peaks within the first 10 s after the photo-chemical release of cGMP, cortical myosin II localization becomes maximal after approximately 30 s. For the myosin II response, our results furthermore indicate a reduced sensitivity in the vegetative as compared to developed cells.

Application of extracellular cAMP to starvation-developed *Dictyostelium* cells results in a transient translocation of myosin II to the cell cortex. An increase in the cytosolic cGMP concentration has long been shown to precede this response.[8,9] Mutants that are unable to produce cGMP because of disrupted guanylyl cyclases display a strongly reduced myosin II translocation leading to impaired chemotaxis. Similar defects were observed in a knockout mutant lacking the cGMP binding protein GbpC, strongly indicating that a cGMP-mediated pathway *via* activation of GbpC controls cortical localization and function of myosin II in chemotactic cells.[12] Our uncaging experiments clearly confirm these earlier results. They provide a direct proof that an increase in the cytosolic cGMP concentration triggers myosin II translocation to the cortex.

While the myosin II response to an intracellular release of cGMP was thus expected, the preceding rapid peak in actin polymerization was not. Interestingly, the timing of the actin and myosin II peaks is in agreement with the responses observed after stimulation with extracellular cAMP.[3] Also here, a sharp peak in actin polymerization within the first seconds after the stimulus is followed by a prolonged myosin translocation that peaks about 20 s later. Furthermore, it has been shown earlier that translocation of myosin II to the cell cortex requires both binding of myosin to intact F-actin structures and motor activity of the myosin heads.[38] This suggests that myosin motor motility drives the translocation. Even though F-actin is required for motor-driven myosin II translocation, no evidence has been reported so far that actin polymerization may be stimulated by the same cGMP-mediated pathway that controls myosin activity. Our present data suggest such a link and indicate that actin polymerization may be triggered by an increase in the intracellular level of cGMP.

How is cGMP linked to actin polymerization in *Dictyostelium*? Several options may be considered. On the one hand, cGMP may activate VASP (vasodilator-stimulated phosphoprotein) that plays an important role in controlling actin-driven processes in cells.[39] VASP was first discovered as a protein phosphorylated in response to elevated cAMP and cGMP in human platelets. It is part of the Ena/VASP family of proteins found in vertebrates, invertebrates, and *Dictyostelium*. Members of the Ena/VASP family are observed in areas of dynamic actin reorganization, for example the leading edge, tips of filopodia, cell–cell contacts, and focal adhesions.[40] They are also involved in axon guidance, phagocytosis, neural tube closure, T cell activation, and attenuation of platelet aggregation.[41] In *D. discoideum*, the homolog DdVASP was found.[39,41] DdVASP expression occurs in vegetative cells and increases with starvation peaking at 8 h.[39] Phosphorylation of VASP is important for its cortical localization and interaction with WASP and WIPa that are key regulators of F-actin organization.[42] Lin and co-workers[42] showed that VASP phosphorylation still occurs in *Dictyostelium* null strains of the PKA catalytic domain (*pka-cat*$^-$) and of guanylyl cyclases (*sgc/gca*$^-$). Furthermore, no VASP phosphorylation was observed in cells treated with membrane-permeable derivatives of cAMP and cGMP. Together, these results suggest that VASP phosphorylation in *Dictyostelium* does not depend on cyclic nucleotides and, thus, is not a likely candidate to explain our experimental observations.

Other candidates to explain the transient increase in actin polymerization that we observed after an intracellular release of cGMP are the cGMP binding proteins GbpC and GbpD. Although the cAMP-induced actin polymerization does not critically rely on these proteins,[20] a parallel pathway that activates the actin machinery *via* cGMP signalling cannot be excluded. In fact, earlier results indicate that GbpD indeed affects actin polymerization.[20] However, even though GbpD contains two cyclic nucleotide binding domains, it was shown that only GbpC exhibits high affinity binding sites for cGMP.[12] Moreover, the flattened and strongly adherent phenotype of GbpD overexpressing cells was also observed in the absence of intracellular cGMP, suggesting that GbpD activity does not depend on cGMP. Nevertheless, based on estimates of the cGMP dissociation constant of GbpD, we cannot rule out that cGMP is regulating GbpD when peak levels in the cytosolic cGMP concentration are reached.[20] Note that with decreasing strength of the intracellular cGMP stimulus, a GbpD mediated actin response should rapidly decay, while the GbpC mediated myosin II response would persist due to the much higher binding affinity of GbpC for cGMP. However, this is not in agreement with our experimental observations. When placing the uncaging laser outside of the cell to reduce the light-induced intracellular release of cGMP, the myosin II response is diminished, while the actin response persists (see Fig. 3C).

Finally, actin polymerization may also be stimulated *via* a cGMP/GbpC mediated pathway, similar to myosin II. GbpC has

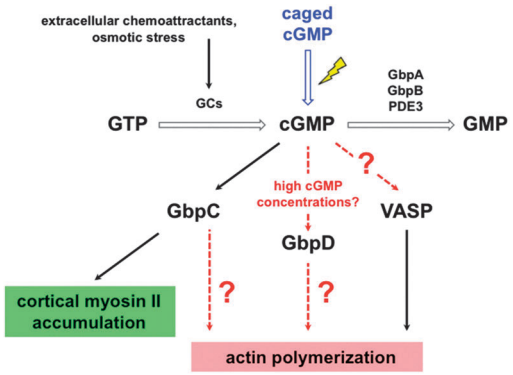

Fig. 5 Cyclic GMP signaling in *D. discoideum*. In blue: manipulation of the intracellular cGMP level by photo-uncaging. In red: hypothetical links of the cGMP pathway to cortical actin polymerization (optional). GTP (guanosine triphosphate), GCs (guanylyl cyclases), GbpA-D (cGMP binding protein A-D), VASP (vasodilator-stimulated phosphoprotein).

been classified as a member of the Roco family of proteins and displays a rich topology of domains.[23,24] Since the substrates that are regulated by active GbpC are not known, it is conceivable that the cGMP/GbpC pathway branches downstream of GbpC to control both myosin and actin activity in the cell cortex. For an overview of the possible signalling interactions, see Fig. 5.

In summary, we have shown for the first time a direct optical live cell measurement of cytoskeletal activity following an intracellular release of cGMP in *Dictyostelium*. As expected, an increase in intracellular cGMP induces myosin II to accumulate in the cortex. Surprisingly, also cortical actin polymerization rises in a sharp transient peak following the cGMP stimulus, independently of cAMP receptor activation and signaling. We have furthermore demonstrated that stray light may limit the localization of photo-uncaging events, even when a focused laser beam is used. In our experiments, intracellular uncaging was initiated even in cases where the uncaging laser was placed outside the cell of interest, highlighting the impact of stray light in this sensitive optical live cell stimulation technique.

Materials and methods

Cell culture and chemicals

AX2-Wild Type (WT) cells were cultured in HL-5 medium (Formedium, Hunstanton, UK). When culturing GFP-Myosin II + LimEΔ-mRFP cells, the selection markers G418 disulfate (Applichem, Darmstardt, Germany) and Blasticidin S hydrochloride (Applichem, Darmstardt, Germany) were added. All experiments were done with cells in Sørensen phosphate buffer (14.6 mM KH_2PO_4 (Merck, Darmstadt, Germany), 2 mM Na_2HPO_4 (Merck, Darmstadt, Germany), pH 6.0). For developed cells, 2×10^6 cells were shaken in buffer for 6 h. cAMP responsiveness was tested by adding a drop of 10^{-4} M cAMP (adenosine 3,5 – cyclic monophosphate, from Sigma-Aldrich, Taufkirchen, Germany) and visualizing LimEΔ translocation to the cortex before each experiment. Other chemicals: DMACM-caged 8-Br-cGMP ((7-dimethylaminocoumarin-4-yl)methyl-8-bromoguanosine-3′,5′-cyclic monophosphate) was purchased from *Biolog* (Bremen, Germany); cGMP (Guanosine 3,5-cyclic monophosphate), Br-cGMP (8-bromoguanosine 3,5-cyclic monophosphate sodium salt), DMAC (7-dimethylamino-4-methyl-coumarin) and dihydroethidium (for fluorescence) were purchased from Sigma-Aldrich, Taufkirchen, Germany.

Laser-induced uncaging of DMACM-caged 8-Br-cGMP

Cells were plated in glass-bottom dishes and incubated in 10 μM caged-cGMP. The lasers used had the following wavelengths: 488 nm argon laser, 561 nm DPSS laser, and a Diode 405-30 laser of 405 nm, which is the photobleaching laser. An area of 21 pixels (circle) inside or outside (next to) the cell was illuminated with 100% photobleaching laser intensity, and a pixel dwell time of 25.21 ms. Images were captured at a rate of one frame per second using an LSM 710 microscope (Carl Zeiss Microimaging, Jena, Germany) with a PlnApo 63x/1.4 Oil DicIII objective.

Dihydroethidium photoactivation control assay

Cells were plated in glass-bottom dishes and incubated, protected from light, for 2 hours in 20 μM Dihydroethidium (Sigma-Aldrich, Taufkirchen, Germany). Cells (AX2-WT) were exposed to a 355 nm laser (Genesis 355-150, Coherent Deutschland, Dieburg, Germany); the fluorescence intensities inside the cells before and after stimulation were measured and plotted as a function of distance from the position of the laser.

Image analysis

Every recorded image sequence was converted into a 3D-array containing the stack of all images with dimensions x, y, t, with t being the number of the subsequent images. First, the background intensity was calculated by averaging over all images, calculating the temporal mean value of every pixel (x, y). From the resulting background image, mean intensity and maximum intensity values were calculated.

The images in the 3D-array were then smoothed by a 3D median filter with a $5 \times 5 \times 5$ pixel cubic mask. After this operation was performed on both color channels, the two channels (for the GFP and for the mRFP images), both being normalized by the maximum intensity from the background image, were added together. To determine the cytosolic and cortical regions of the cell, we generated two masks. First, we applied a threshold to the filtered image of 40% of the mean intensity value retrieved from the background image. We then eroded the binarized image by a zone of 16 pixels in diameter. The remaining part represents the cytosol, while the difference of the eroded and the non-eroded binarized images provides the mask for the cortical region of the cell. Both masks were then applied to the sequence of original images. The mean fluorescence intensities were computed separately for the sequence of both the cell cortex and cytosol images. To characterize the cytoskeletal response, the ratio of both intensities was plotted as a function of time. The image analysis was done with a custom-made MATLAB program (MATLAB 7.5, Mathworks, Ismaning, Germany). For more information on the image analysis, see Anielski *et al.*[31]

Acknowledgements

We are grateful to Kirsten Krüger for assistance and thank Hellen Ishikawa-Ankerhold and Günther Gerisch for discussions. We thank Bernd Walz for generous access to his Zeiss LSM 710 confocal microscope and Otto Baumann for continuous help in operating the microscope. Financial support by the Deutsche Forschungsgemeinschaft is gratefully acknowledged (DFG BE 3978/3-1).

Notes and references

1 S. Yumura and Y. Fukui, *Nature*, 1985, **314**, 194–196.
2 R. Kessin, *Dictyostelium: Evolution, Cell Biology, and the Development of Multicellularity*, 2001.
3 M. Etzrodt, H. C. F. Ishikawa, J. Dalous, A. Muller-Taubenberger, T. Bretschneider and G. Gerisch, *FEBS Lett.*, 2006, **580**, 6707–6713.
4 G. Liu, H. Kuwayama, S. Ishida and P. C. Newell, *J. Cell Sci.*, 1993, **106**, 591–596.
5 B. Wurster, K. Schubiger, U. Wick and G. Gerisch, *FEBS Lett.*, 1977, **76**, 141–144.
6 J. M. Mato, F. A. Krens, P. J. M. V. Haastert and T. M. Konijn, *Proc. Natl. Acad. Sci. U. S. A.*, 1977, **74**, 2348–2351.
7 F. M. Ross and P. C. Newell, *J. Gen. Microbiol.*, 1981, **127**, 339–350.
8 G. Liu and P. C. Newell, *J. Cell Sci.*, 1988, **90**, 123–129.
9 G. Liu and P. C. Newell, *J. Cell Sci.*, 1991, **98**, 483–490.
10 G. Liu and P. C. Newell, *J. Cell Sci.*, 1994, **107**, 1737–1743.
11 M. A. De la Roche, J. L. Smith, V. Betapudi, T. T. Egelhoff and G. P. Cote, *J. Muscle Res. Cell Motil.*, 2002, **23**, 703–718.
12 L. Bosgraaf, H. Russcher, J. L. Smith, D. Wessels, D. R. Soll and P. J. M. Van Haastert, *Embo J.*, 2002, **21**, 4560–4570.
13 H. Kuwayama and P. J. M. Van Haastert, *FEBS Lett.*, 1998, **424**, 248–252.
14 H. Kuwayama, M. Ecke, G. Gerisch and P. J. M. VanHaastert, *Science*, 1996, **271**, 207–209.
15 G. Gerisch and B. Hess, *Proc. Natl. Acad. Sci. U. S. A.*, 1974, **71**, 2118–2122.
16 P. G. Charest and R. A. Firtel, *Biochem. J.*, 2007, **401**, 377–390.
17 F. Marks, U. Klingmüller and K. M. Decker, *Cellular signal processing*, 2009.
18 J. M. Goldberg, L. Bosgraaf, P. J. M. Van Haastert and J. L. Smith, *Proc. Natl. Acad. Sci. U. S. A.*, 2002, **99**, 6749–6754.
19 M. Meima, K. E. Weening and P. Schaap, *J. Biol. Chem.*, 2003, **278**(16), 14356–14362.
20 L. Bosgraaf, A. Waijer, R. Engel, A. J. W. G. Visser, D. Wessels, D. Soll and P. J. M. Van Haastert, *J. Cell Sci.*, 2005, **118**, 1899–1910.
21 A. Kortholt, P. Bolourani, H. Rehmann, I. Keizer-Gunnink, G. Weeks, A. Wittinghofer and P. J. M. Van Haastert, *Mol. Biol. Cell*, 2010, **21**, 936–945.
22 D. M. Veltman and P. J. M. Van Haastert, *J. Cell Sci.*, 2008, **121**, 120–127.
23 W. N. Van Egmond and P. J. M. Van Haastert, *Eukaryotic Cell*, 2010, **9**, 751–761.
24 W. N. Van Egmond, A. Kortholt, K. Plak, L. Bosgraaf, S. Bosgraaf, I. Keizer-Gunnink and P. J. M. Van Haastert, *J. Biol. Chem.*, 2008, **283**, 30412–30420.
25 I. Marín, W. N. Van Egmond and P. J. M. Van Haastert, *FASEB J.*, 2008, **22**, 3103–3110.
26 A. Kortholt, W. N. Van Egmond, K. Plak, L. Bosgraaf, I. Keizer-Gunnink and P. J. M. Van Haastert, *J. Biol. Chem.*, 2012, **287**, 2749–2758.
27 A. Ishihara, K. Gee, S. Schwartz, K. Jacobson and J. Lee, *Biotechniques*, 1997, **23**, 268–274.
28 G. C. R. Ellis-Davies, *Nat. Methods*, 2007, **4**, 619–628.
29 N. Schneider, I. Weber, J. Faix, J. Prassler, A. Müller-Taubenberger, J. Kohler, E. Burghardt, G. Gerisch and G. Marriott, *Cell Motil. Cytoskeleton*, 2003, **56**, 130–139.
30 V. Hagen, S. Frings, B. Wiesner, S. Helm, U. B. Kaupp and J. Bendig, *ChemBioChem*, 2003, **4**, 434–442.
31 A. Anielski, E. K. B. Pfannes and C. Beta, *J. Comput. Interdiscip. Sci.*, 2012, **3**, 99–106.
32 J. C. Brasen, S. Dewitt and M. B. Hallett, *Biophys. J.*, 2010, **98**, L25–L27.
33 G. Dorman and G. D. Prestwich, *Trends Biotechnol.*, 2000, **18**, 64–77.
34 C. Beta, D. Wyatt, W. J. Rappel and E. Bodenschatz, *Anal. Chem.*, 2007, **79**, 3940–3944.
35 C. Westendorf, J. Negrete, A. J. Bae, R. Sandmann, E. Bodenschatz and C. Beta, *Proc. Natl. Acad. Sci. U. S. A.*, 2013, **110**, 3853–3858.
36 V. Hagen, J. Bendig, S. Frings, B. Wiesner, B. Schade, S. Helm, D. Lorenz and U. Benjamin Kaupp, *J. Photochem. Photobiol., B*, 1999, **53**, 91–102.
37 V. Hagen, J. Bendig, S. Frings, T. Eckardt, S. Helm, D. Reuter and U. Benjamin Kaupp, *Angew. Chem., Int. Ed.*, 2001, **40**, 1045–1048.
38 S. Levi, M. V. Polyakov and T. T. Egelhoff, *Cell Motil. Cytoskeleton*, 2002, **53**, 177–188.
39 Y. H. Han, C. Y. Chung, D. Wessels, S. Stephens, M. A. Titus, D. R. Soll and R. A. Firtel, *J. Biol. Chem.*, 2002, **277**, 49877–49887.
40 M. Krause, E. W. Dent, J. E. Bear, J. J. Loureiro and F. B. Gertler, *Annu. Rev. Cell Dev. Biol.*, 2003, **19**, 541–564.
41 A. V. Kwiatkowski, F. B. Gertler and J. J. Loureiro, *Trends Cell Biol.*, 2003, **13**, 386–392.
42 W. H. Lin, S. E. Nelson, R. J. Hollingsworth and C. Y. Chung, *Cytoskeleton*, 2010, **67**, 259–271.